Thermomagnetic history effects in $SmMn_2Ge_2$

Sujeet Chaudhary,[1,*] M. K. Chattopadhyay,[1] Kanwal Jeet Singh,[1] S. B. Roy,[1] P. Chaddah,[1] and E. V. Sampathkumaran[2]
[1]*Low Temperature Physics Laboratory, Centre for Advanced Technology, Indore 452 013, India*
[2]*Tata Institute of Fundamental Research, Homi Bhabha Road, Colaba, Mumbai 400 005, India*
(Received 19 March 2002; published 12 July 2002)

The intermetallic compound $SmMn_2Ge_2$, displaying multiple magnetic phase transitions, is investigated in detail for its magnetization behavior near the 145-K first-order ferromagnetic-to-antiferromagnetic transition occuring on cooling, in particular, for thermomagnetic history effects in the magnetization data. The most unusual finding is that the thermomagnetic irreversibility, $[=M^{FCW}(T)-M^{ZFC}(T)]$ at 135 K is higher in intermediate magnetic-field strengths. By studying the response of the sample (i.e., thermomagnetic irreversibility and thermal hysteresis) to different histories of application of magnetic field and temperature, we demonstrate how the supercooling and superheating of the metastable magnetic phases across the first-order transition at 145 K contribute to overall thermomagnetic irreversibility.

DOI: 10.1103/PhysRevB.66.014424 PACS number(s): 64.60.My, 72.15.Jf, 64.70.Kb

I. INTRODUCTION

There has been a continued interest in the past decade in understanding the magnetization behavior of the body-centered tetragonal rare-earth transition-metal germanides and silicides (RMn_2Ge_2 and RMn_2Si_2). Various kinds of magnetic phase transitions, viz., paramagnetic (PM) to ferromagnetic (FM), PM to antiferromagnetic (AFM), FM to AFM, AFM to FM, or the ferrimagnetic state (at low temperature, T) can be observed in different compounds belonging to this class of materials.[1–17] The unit cell in these compounds consists of a layered structure . . . -Mn-Mn-R-Ge(or Si)-R-Mn-Mn- . . . stacked along the c axis. Within the ab plane, the Mn-Mn interaction is FM-like for all temperatures below the highest-ordering temperature. It is known that in all the RMn_2Ge_2 and RMn_2Si_2 compounds, the various properties including magnetization (M) are strongly dependent on the intralayer Mn-Mn distance, $d^a_{Mn\text{-}Mn}$ (Ref. 2). It has been established that there exists a critical value of $d^a_{Mn\text{-}Mn}$ below (above) which the Mn spins in one FM layer interact antiferromagnetically (ferromagnetically) with those in the neighboring FM layer.[2] Among the various members of the entire family, the compound $SmMn_2Ge_2$ is unique, in the sense that the intralayer $d^a_{Mn\text{-}Mn}$ is very close to the critical value of 2.84 Å at room temperature.[2,3] Accordingly, significant structural distortions occur in the unit cell of $SmMn_2Ge_2$ as one varies temperature in the range of 360 to 5 K. With a PM-to-FM transition around 350 K (i.e., T_c), these distortions leads to (i) an intermediate-T FM-to-AFM transition around 145 K (T_1), and (ii) a low-T AFM-to-reentrant-FM transition near 100 K (T_2).[2,6] In addition, the easy axis in $SmMn_2Ge_2$ changes from $\langle 001\rangle$ above ≈ 145 K to $\langle 110\rangle$ below ≈ 100 K.[2,6]

The intermediate AFM regime can undergo a metamagnetic transition for magnetic-field strengths, $H \approx 5$ kOe, by which the alternate antiparallel spin configuration of the FM layers is transformed to a parallel one.[7–10] Neutron scattering,[11] NMR[12] and Mossbauer[13] studies have revealed that the magnetic structure of each magnetic phase possess a noncollinear arrangement of spins. Later, a thorough neutron-scattering investigation[14] on a sample containing isotopically enriched Sm revealed the existence of much more complicated cone structures in the AFM as well as low-T reentrant FM regimes. This ternary compound $SmMn_2Ge_2$ has gained further interest due to the observed giant magnetoresistance (GMR) associated with the AFM phase.[7–9,15,16] Magnetoresistance of varying magnitude from 8% to about 16% was reported in these studies. Technologically, this is interesting since most GMR materials are artificially grown as thin-film multilayers.

At this juncture, we would like to recall that we reported[18–20] the thermomagnetic history effects across the first-order FM-to-AFM transition in polycrystalline $Ce(Fe_{0.96}Al_{0.04})_2$. It was shown that the supercooling and superheating of two magnetic phases across the first-order transition (FOT) leads to metastable behavior which resulted in the thermomagnetic irreversibility (TMI) that was found to increase with the increase in H, in sharp contrast with the TMI observed, say, for example, in spin-glass[21] and long-range magnetically ordered systems[22,23] which gets suppressed with the increase in H. In particular, it was found that both M and magnetoresistivity (ρ) at any (T,H) point below the Néel temperature (T_N) were strongly history dependent. Although all the generic features associated with the FOT were observed in $Ce(Fe_{0.96}Al_{0.04})_2$, the superheating signatures were quite subtle compared with those associated with supercooling.[18–20] In this context, the compound $SmMn_2Ge_2$ provides an unique opportunity to probe the aspect of TMI in the view of two first order transitions, as it has been established that both the transitions—at T_1, and T_2—are first order in nature.[6,8,17] This system thus is a natural choice for observing all the characteristics of a FOT (including superheating) as we approach the AFM regime (displaying a negligible moment relative to the FM state) both while heating from the low-T FM regime as well as while cooling from the high-T FM regime. We thus demonstrate through TMI measurements the observation of the metastable phases of both kinds (i.e., supercooled and superheated) so clearly in $SmMn_2Ge_2$. In this paper, we present the thermomagnetic history effects observed on variation of field and temperature across the 145-K first-order transition in $SmMn_2Ge_2$. Ther-

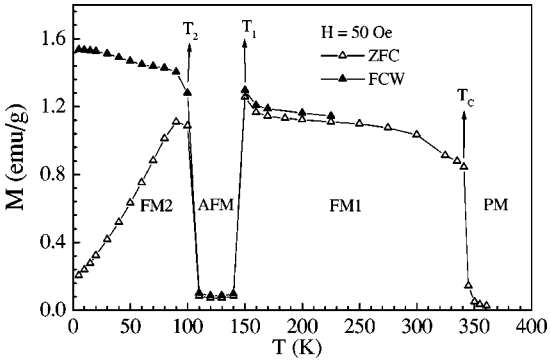

FIG. 1. M vs T plot of $SmMn_2Ge_2$ sample in presence of 50-Oe field recorded in ZFC (open triangles) and FCW (filled triangles) protocols covering the 4.5-to-360-K T range. The different magnetically ordered phases are labeled FM1, AFM, and FM2 in their respective T regimes. Also marked in figure are the transitions, viz., T_c, T_1, and T_2 separating these different magnetic phases. See text for more details.

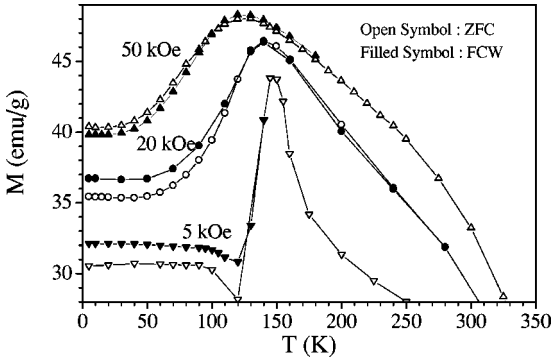

FIG. 2. Effect of magnetic-field strength on the thermomagnetic irreversibility observed between the ZFC- (open symbols) and FCW- (filled symbols) magnetization data recorded between 4.5 and 360 K in $SmMn_2Ge_2$; $H=5$ kOe (inverted triangles), 20 kOe (circles), and 50 kOe (triangles).

momagnetic history effects associated with the low-temperature transition (i.e., at ≈ 100 K) in this compound are still under investigation, and are not addressed in this paper.

II. EXPERIMENTAL DETAILS

Polycrystalline samples of $SmMn_2Ge_2$ were prepared by argon-arc melting. Details of sample preparation and characterization can be found in Ref. 15. The M vs T and/or H data have been recorded using a commercial superconducting quantum interference device (SQUID) magnetometer (model MPMS5) with a scan length of 4 cm. The measurement of M was done in three different experimental protocols, viz., zero-field cooling (ZFC), field cooled cooling (FCC), and field cooled warming (FCW). These protocols are explained in detail in Ref. 19.

III. RESULTS AND DISCUSSION

Before we present the detailed results on thermomagnetic history effects across T_1, we would like to discuss the M vs T as well as M vs H behavior, to serve as a prelude to interpret TMI data. Figure 1 shows the M vs T plot for the $SmMn_2Ge_2$ sample recorded in a low field of 50 Oe both in ZFC and FCW protocols. The PM-to-FM transition takes place at $T_c \approx 345$ K. This high-T FM phase continues down to $T_1 \approx 145$ K, below which the M vs T curve displays a sudden loss of M thereby entering into an AFM regime, which persists down to ≈ 100 K. Below this T, which we refer to as T_2, the magnetization once again increases due to the formation of the (low-T) reentrant FM phase. (Henceforth, these two FM phases existing at high and low T will be represented by FM1 and FM2, respectively.) It may be noted in passing that the high-T FM1 phase (extending over a T range from 145 to 345 K) displays a concave curvature for $T<180$ K, in contrast to a typical M vs T behavior represented by Brillouin function. A large TMI [i.e., $M^{FCW}(T) \neq M^{ZFC}(T)$] is distinctly observed below 100 K. Conventionally, such a TMI in M^{FCW} and M^{ZFC} is commonly taken as the fingerprint of spin-glass behavior.[21] However, it is now established that long-range magnetically ordered systems (i.e., FM, AFM, etc.) can also show significant TMI in their M vs T data,[22,23] which arises mainly from hindrance to domain rotation caused by the magnetocrystalline anisotropy and/or domain-wall pinning effects. One may recall that when TMI arises due to these domain-related effects, it gets suppressed with an increase in H. Thus, the small TMI in the FM1 phase of $SmMn_2Ge_2$ above 145 K (despite the low field of 50 Oe) is definitely indicative of relatively small domain-wall pinning effects. In addition, in view of highly anisotropic magnetization behavior of $SmMn_2Ge_2$, the small TMI in the FM1 phase also suggests that either there is a relatively small magnetocrystalline anisotropy or there is some preferential orientation of $\langle 001 \rangle$ grains parallel to applied H in this polycrystalline sample. However, on the basis of the data of Fig. 1 alone, it is not possible to decipher which of the above two factors is causing the small TMI observed above T_1.

To know about the H dependence of the TMI behavior in $SmMn_2Ge_2$, we show in Fig. 2 the M vs T plots for H, namely, 5 kOe, 20 kOe, and 50 kOe. We find the following:

(i) Instead of loss of magnetization as observed at low H (see Fig. 1) in the AFM regime, a ''dip'' like feature is now observed in the M vs T plot for $H=5$ kOe, indicating that the AFM regime is narrowed down in high H. We also want to draw the reader's attention to the fact that relative to the TMI in small H (see Fig. 1), the increase of H to a moderate value, for instance, 5 kOe, has almost smeared out the T_2 transition, whereas the T_1 transition is less affected qualitatively. Furthermore, in presence of high fields ($H \geqslant 5$ kOe), the moment in the FM1 phase is distinctly larger than that in the FM2 phase, which is in sharp contrast with the situation at 50 Oe (see Fig. 1). At even higher H, the M vs T plots do not show any dip in magnetization at the T_2 transition (i.e., for both $H=20$ kOe and 50 kOe). Instead, magnetization (in $H=50$ kOe) rises with T right from $T>30$ K.

(ii) The TMI (see, e.g., magnetization at 5 K) decreases as one goes from 50 Oe (Fig. 1) to 20 kOe (Fig. 2). However, at 50 kOe, we find that TMI has a different sign, i.e.,

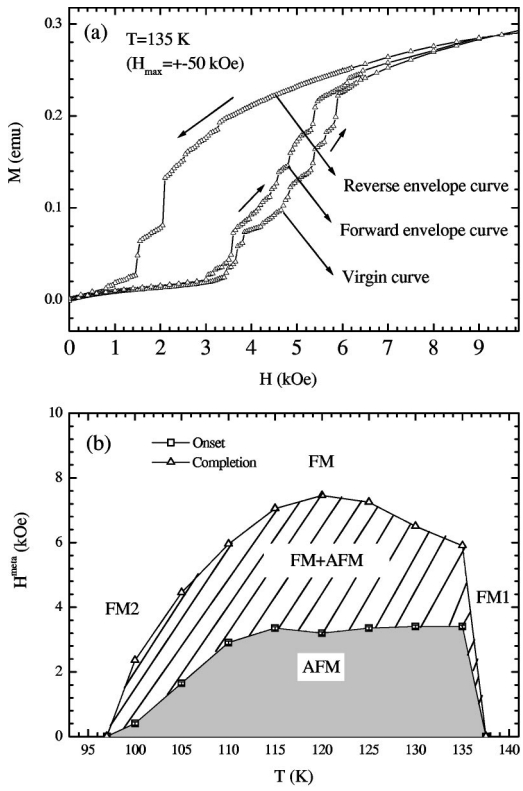

FIG. 3. (a) The M vs H curve at 135 K (which is reached in zero field on cooling from above T_c) showing the hysteresis between the forward- and reverse-envelope cycles recorded between $H=+50$ kOe and $H=-50$ kOe. Note that the virgin magnetization branch lies outside the complete hysteretic loop. The rise in M at ≈ 3 kOe is due to the field-induced AFM-to-FM transition which takes place through successive random jumps in M until it is finally completed at ≈ 6 kOe. See text for further details. (b) The magnetic phase diagram of the investigated $SmMn_2Ge_2$ sample highlighting the completely AFM regime separated from the completely FM regime through a mixed-phase regime (i.e., comprising AFM and FM fractions). The various points along the two boundaries on either side of this mixed-phase regime are obtained by inferring the onset (squares) and completion (triangles) of a metamagnetic (i.e., AFM-to-FM) transition at different temperatures within the AFM regime [i.e., from various M-H loops, like, e.g., Fig. 3(a) for $T=135$ K].

$M^{FCW}(T) < M^{ZFC}(T)$. This change in sign of TMI at higher H is quite anomalous, the origin of which is unclear at present.

(iii) The peak in M (observed in both FCW as well as ZFC protocols) shifts to a lower T with the increase in strength of H, and this implies a complex intermediate-temperature magnetic phase at higher H.

As mentioned in the preceding discussion, in order to identify these critical fields of metamagnetic transition $H^{meta}(T)$, we recorded various isothermal M vs H plots within the AFM regime. Figure 3(a) shows one such plot at 135 K, in which (i) the initial M vs H curve recorded after reaching the 135-K point strictly in a ZFC manner from above T_c (i.e., the *virgin curve*), (ii) a portion of the H-reversal cycle from the maximum 50 kOe down to -50 kOe through 0 kOe (i.e., a *reverse-envelope curve*), and (iii) a portion of the field ascending M-H curve initiated after field excursion from -50 kOe (i.e., a *forward-envelope curve*) are shown for the $SmMn_2Ge_2$ sample.

A slow increase in M until about 3 kOe is consistent with the low-field AFM state in the present $SmMn_2Ge_2$ sample at 135 K. With a further increase in H, a number of jumps in M are clearly resolved until about 6 kOe along the virgin M-H branch [Fig. 3(a)]. At higher-field strengths, the observation of usual saturationlike behavior (typical of a FM state) indicates the completion of a field-induced AFM-to-FM transition in the $SmMn_2Ge_2$ sample. The observed randomness in both the magnitude as well as the position of these various jumps [which are as much as ten in number in the present case of the $SmMn_2Ge_2$ sample, see Fig. 3(a)] may be attributed to a distribution of H^{meta} due to possible inhomogenieties/disorder in the polycrystalline sample together with the high anisotropy of $SmMn_2Ge_2$. From the first and the last jumps in the virgin M vs H curve, one can identify the critical field for the onset and completion of metamagnetic transition at 135 K. In Fig. 3(b), we plot these two critical fields as a function of T covering the entire AFM regime. We shall refer to this phase diagram when we discuss our measurements to look for metastable (supercooled/superheated) states by varying T in fixed H. Finally, it is worth noting that the virgin M vs H curve lies anomalously outside the full hysteretic loop obtained by cycling the field between $+50$ kOe and -50 kOe [see Fig. 3(a)]. A similar anomalous virgin curve was observed in the M vs H and ρ vs H data of $Ce(Fe_{0.96}Al_{0.04})_2$.[18–20]

We stress here that the $M^{FCW}(T)$ data presented in Fig. 1 and Fig. 2 have been recorded after cooling the sample (in the presence of respective H's) across the *two* FOT's [and not one FOT, as reported in Refs. 18–20 in the $Ce(Fe_{0.96}Al_{0.04})_2$ system]. We further point out here that great care is required when dealing with systems such as the present $SmMn_2Ge_2$ sample, since metastabilities across both the first-order transitions (i.e., FM1 to AFM, and AFM to FM2) may mask the magnetic character of that particular phase (due to the supercooling and superheating of various phases across the two transitions).[24] Thus, the TMI effects in $SmMn_2Ge_2$ may be different not only from those encountered in only FM- or only AFM-ordered compounds,[22,23] but also from the TMI observed across a single FOT from FM to AFM as discussed in Refs. 18–20. In this paper, we will focus on TMI effects only across the T_1 transition. To limit the contributions to the overall TMI (say, near the transition temperature) arising from the metastable effects related to domain pinning/hindrance, the strength of H should be small enough so as not to drive the AFM state into a FM state while preparing the field cooled state from, say, at 135 K.

In Fig. 4, we show the effect of the strength of H on the TMI (near the T_1 transition) obtained from the M vs T plots which have been recorded while warming the sample (i) after cooling in zero field from above T_c to 120 K (thereby ensuring the initial phase at 120 K to be purely AFM) at which the appropriate field is applied (i.e., ZFC protocol), and (ii) from 135 K which the sample reached in the presence of H when

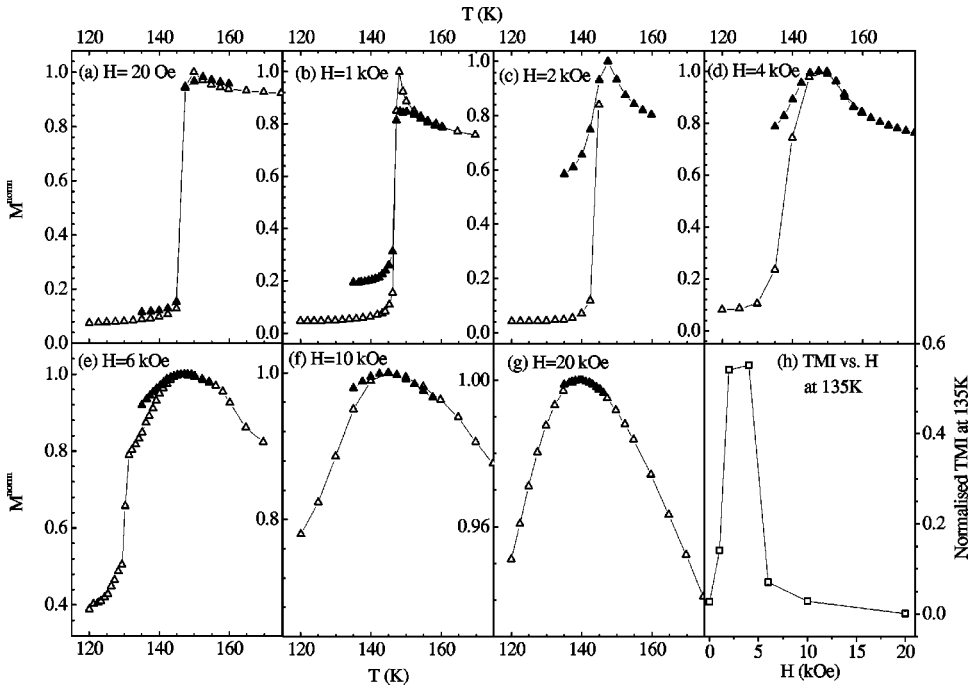

FIG. 4. (a)–(g) The effect of field strength on the TMI between the ZFC (open symbols) and FCW (filled symbols) M vs T runs. While ZFC runs for each field are initiated from 120 K which the sample reached in zero field on cooling from above T_c, the FCW runs have been initiated from 135 K which the sample reached when carefully cooled after the completion of the ZFC run to more than 200 K; (a) $H=20$ Oe, (b) 1 kOe, (c) 2 kOe, (d) 4 kOe, (e) 6 kOe, (f) 10 kOe, and (g) 20 kOe. Note that in order to have a proper comparison, the magnetization data is normalized with respect to the peak value observed near the T_1 transition. (h) The thermomagnetic irreversibility at 135 K [i.e., $M^{norm,\ FCW}(135\ \mathrm{K},H)$-$M^{norm,\ ZFC}(135\ \mathrm{K},H)$] as a function of applied field strength.

cooled from a temperature T_0 $(>T_1)$ (i.e., FCW protocol). [T_0 is the temperature up to which the sample is warmed while recording $M^{ZFC}(T)$ data as explained in step (i) above.]

Note that the M vs T plots in Figs. 4(a)–4(g) are normalized to their maximum value at the transition T_1, to allow a proper comparison of the effect of the strength of applied field on the TMI. It can be seen that the TMI observed below T_1 [i.e., $M^{FCW}(135\ \mathrm{K})$- $M^{ZFC}(135\ \mathrm{K})$] rises with the increase in H from 20 Oe to 2 kOe [see Fig. 4(h)]. As discussed above, such a TMI between ZFC and FCW—i.e., increasing with field—indicates (at first-place) the first order nature of the magnetic transition taking place at T_1, rather than having an origin due to domain-related behavior wherein the TMI gets suppressed with the increase in H.[22,23] However, with a further increase in H, the drastic decrease of TMI at 135 K is observed. It thus turns out from the foregoing data that TMI at intermediate H (i.e., $\approx 2-4$ kOe) is higher than the TMI observed both in low (i.e., 20 Oe and 1 kOe) or high (i.e., 6, 10, and 20 kOe) fields. This is remarkably a peculiar finding. We now discuss the possible origin of this behavior.

We note from Fig. 3(b), that the sample undergoes a complete metamagnetic transition at 120 K by ≈ 7.5 kOe field [see Fig. 3(b)], with the result that along the ZFC warming M vs T curve [open data symbols in Figs. 4(a)–4(g)], the sample is completely in a FM state for $H=10$ kOe and 20 kOe, and partly in AFM and FM states for 3.2 kOe$<H<7.5$ kOe. The TMI increasing with the increase in H from 20 Oe to 2 kOe should predominantly be due to the superheating of the (metastable) AFM phase while warming along the ZFC protocol, and also due to the additional metastability in $M^{FCW}(T)$ along the FCW run (filled data symbols in Figs. 4(a)–4(g) as there is always a probability that a finite fraction of the FM1 phase may get supercooled down to 135 K (the starting T of the FCW run). This initial trend of TMI (i.e., increasing with H, and consistent with the arguments of Chaddah and Roy[25]) is also identical to the one observed in the $M(T,H)$ and $\rho(T,H)$ data of $Ce(Fe_{0.96}Al_{0.04})_2$ exhibiting a FOT from FM to AFM at ≈ 100 K.[18–20] The TMI in $SmMn_2Ge_2$ for $H\approx 4$ kOe or higher may be attributed to arise from both the metastable effects associated with domain-related causes, as well as the metastable effects associated with the FOT at T_1. This is so because for $H\geqslant 4$ kOe (but $\leqslant 7.5$ kOe), the sample also consists of a finite fraction of FM1 phase [see Fig. 3(b)] along the ZFC cycle right from 120 K onwards, which would result in higher M^{ZFC} below $\approx T_1$, thereby resulting in a small TMI as is experimentally observed in Figs. 4(d) and 4(e). This finite FM fraction in ZFC would also contribute in a further reduction in TMI with increase in H, becasue of the known supression of TMI arising due to domain-related effects with an increase in H.[22,23] On the other hand, given the first-order nature of the transition at T_1, one may still argue that the FCW data of the M vs T plot (for 10 kOe or higher) could still result due to the supercooling of the high-T FM1 phase. We shall defer this question for time being, and point out that (i) the thermal hysteresis at the onset of the transition while

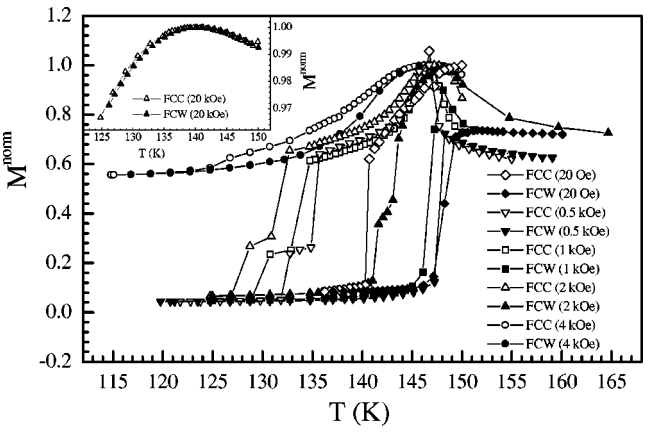

FIG. 5. The normalized magnetic moment as a function of temperature for $SmMn_2Ge_2$ while cooling in the presence of field from 150 K down to a temperature between 115–125 K (i.e., FCC protocol), and subsequent warming to above 150 K (i.e., FCW protocol). Main panel: $H=20$ Oe (diamonds), 0.5 kOe (inverted triangles), 1 kOe (squares), 2 kOe (triangles), and 4 kOe (circles). The open and filled symbols, respectively, represent the FCC and FCW data. The inset shows the thermal cycling (i.e., FCC and FCW runs) for $H=20$ kOe. Within the error in temperature measurements ($\leqslant 0.5$ K), there is no hysteresis in FCC and FCW data for this high-field strength (i.e., 20 kOe).

cooling and warming in the presence of field,[26] and (ii) its dependence on H are both instructive for knowing the dominance of metastable effects associated with any FOT. In the next section, we shall present results of H dependence of thermal hysteresis across the T_1 transition.

In Fig. 5, we show the results of thermal cycling of the $SmMn_2Ge_2$ sample across the T_1 transition in the presence of different field strengths. [It should once again be noted that the M vs T data for different H's (for both FCC as well as FCW protocols) is normalized with respect to the highest M value observed along the FCC curve.] For each H, we first brought the sample to 150 K in a ZFC manner from above T_c, then the field is applied and FCC data is first collected down to 120 K followed by recording the FCW data by warming the sample up to and above T_1. Akin to the multiple jumps seen in the M vs H curves within the AFM regime [Fig. 3(a)], more than one jump in M is also observed in these thermal cyclings as well. A significant amount of thermal hysteresis is visible for all the field strengths up to $H=4$ kOe. (This presence of thermal hysteresis[26] itself indicates the first-order nature of the T_1 transition.) However, the absence of thermal hysteresis between the FCC and FCW curves recorded in high magnetic-field strengths (see the inset to Fig. 5 for the $H=20$-kOe case) immediately confirms that the T_1 transition is a second-order transition in the presence of higher H. In our opinion, this transition at $H=20$ kOe involves a gradual transformation of the FM1 state with a particular easy axis to another FM state (possibly FM2-like) with a different easy axis. (That is, the transition in higher H is associated with the change in anisotropy in $SmMn_2Ge_2$ near 145 K.)

The amount of thermal hysteresis (near the midpoint of the total magnetization change at the T_1 transition) increases from about ≈ 7 K in 20 Oe, and to ≈ 12 K at 0.5 kOe, to ≈ 13 K at 1 kOe, and then decreases to ≈ 10 K at 2 kOe, and then to ≈ 4 K at 4 kOe. The initial increase of thermal hysteresis from 20 Oe to 1 kOe is consistent within the picture of FOT.[25] This is explained as follows: while cooling (warming) the sample in the presence of H from 150 K (120 K) a finite fraction of the high- (intermediate-) temperature FM1 (AFM) phase supercools (superheats) below (above) T_1 down (up) to the lower-T (higher-T) metastable limit $T^*(H)[T^{**}(H)]$, which is the temperature at which the hysteresis collapses on the lower-T (higher-T) side.[24] Within this FOT picture, it is very necessary that the hysteretic regime in $SmMn_2Ge_2$ should also widen with an increase in H. The results shown in Fig. 5 support this beyond any doubt until 1 kOe. Although a further increase in H suppresses the hysteresis, the presence of hysteresis above $H \geqslant 1$ kOe itself is indicative of a first-order-like transition up to 4 kOe[26] (or up to the H, where one could still observe the hysteresis in $SmMn_2Ge_2$). In field strengths $H \geqslant 1$ kOe, the reduction in the thermal hysteresis with H could be associated with the varying fractions of AFM and FM phases in $SmMn_2Ge_2$, while traversing the phase coexistence regime [see Fig. 3(b)] on either side (during the FCC and FCW runs) or to the distribution in $H^{meta}(T)$ in the sample.

IV. CONCLUSION

We have probed the thermomagnetic history effects in a compound, viz., $SmMn_2Ge_2$, exhibiting two first-order magnetic transitions. We have mainly focused the present study on a FM-to-AFM transition occuring around 145 K in $SmMn_2Ge_2$. The most unusual finding is that higher TMI is observed at intermediate field strengths. The results reveal that there are two kinds of metastable effects giving rise to the observed TMI in $SmMn_2Ge_2$: (i) the metastable effects associated with a first-order transition (i.e., supercooling and superheating) dominate at lower fields, and (b) the metastable effects resulting from the hindrance to the domain rotation process caused due to the high magnetocrystalline anisotropy and/or due to the pinning of domain walls at lattice defects dominate above 4 kOe.

*Corresponding author. Present permanent address: Department of Physics, Indian Institute of Technology Delhi, Hauz Khas, New Delhi 110 016, India. FAX: +91-11-6581114. Email address: sujeetc@physics.iitd.ernet.in

[1] K.S.V.L. Narasimhan, V.U.S. Rao, R.L. Bergner, and W.E. Wallace, J. Appl. Phys. **46**, 4957 (1975).

[2] H. Fujii, T. Okamoto, T. Shigeoka, and N. Iwata, Solid State Commun. **53**, 715 (1985).

[3] A. Szytula and J. Leciejewicz, in *Handbook on the Physics and Chemistry of Rare Earths*, edited by K.A. Gschneidner and L. Eyring (Elsevier Science, New York, 1989), Vol. 12, p. 133; A. Szytula, J. Alloys Compd. **178**, 1 (1992).

[4] H. Fujii, M. Isoda, T. Okamoto, T. Shigeoka, and N. Iwata, J. Magn. Magn. Mater. **54-57**, 1345 (1986).
[5] J.E. McCarthy, J.A. Duffy, C. Detlefs, M.J. Cooper, and P.C. Canfield, Phys. Rev. B **62**, R6073 (2000).
[6] E.M. Gyorgy, B. Batlogg, J.P. Remeika, R.B. van Dover, R.M. Fleming, H.E. Bair, G.P. Espinosa, A.S. Cooper, and R.G. Maines, J. Appl. Phys. **61**, 4237 (1987).
[7] J.H.V.J. Brabers, K. Bakker, H. Nakotte, F.R. de Boer, S.K.J. Lenczowski, and K.H.J. Buschow, J. Alloys Compd. **199**, L1 (1993).
[8] R.B. van Dover, E.M. Gyorgy, R.J. Cava, J.J. Krajewski, R.J. Felder, and W.F. Peck, Phys. Rev. B **47**, 6134 (1993).
[9] J.H.V.J. Brabers, A.J. Nolten, F. Kayzel, S.K.J. Lenczowski, K.H.J. Buschow, and F.R. de Boer, Phys. Rev. B **50**, 16 410 (1994).
[10] J.H.V.J. Brabers, K.H.J. Buschow, and F.R. de Boer, Phys. Rev. B **59**, 9314 (1999).
[11] G. Venturini, R. Welter, E. Ressouche, and B. Malaman, J. Alloys Compd. **223**, 101 (1995); G. Venturini, R. Welter, E. Ressouche, and B. Malaman, J. Magn. Magn. Mater. **150**, 197 (1995); G. Venturini, B. Malaman, and E. Ressouche, J. Alloys Compd. **237**, 61 (1996).
[12] J.S. Lord, P.C. Riedi, Cz. Kapusta, and K.H.J. Buschow, Physica B **206-207**, 383 (1995); J.S. Lord, P.C. Riedi, G.J. Tomka, Cz. Kapusta, and K.H.J. Buschow, Phys. Rev. B **53**, 283 (1996).
[13] I. Nowik, Y. Levi, I. Felner, and E.R. Bauminger, J. Magn. Magn. Mater. **147**, 373 (1995).
[14] G.J. Tomka, C. Ritter, P.C. Riedi, Cz. Kapusta, and W. Koccemba, Phys. Rev. B **58**, 6330 (1998).
[15] E.V. Sampathkumaran, P.L. Paulose, and R. Mallik, Phys. Rev. B **54**, R3710 (1996).
[16] R. Mallik, E.V. Sampathkumaran, and P.L. Paulose, Physica B **230-232**, 731 (1997); E.V. Sampathkumaran, R. Mallik, P.L. Paulose, and Shubam Majumdar, Phys. Lett. A **268**, 123 (2000).
[17] G.J. Tomka, Cz. Kapusta, C. Ritter, P.C. Riedi, R. Cywinski, and K.H.J. Buschow, Physica B **230-232**, 727 (1997); M. Slaski, T. Laegrid, K. Fossheim, Z. Tomkowicz, and A. Szytula, J. Alloys Compd. **178**, 249 (1995); G. Venturini, *ibid.* **232**, 133 (1996).
[18] M. Manekar, S. Chaudhary, M.K. Chattopadhyay, K.J. Singh, S.B. Roy, and P. Chaddah, Phys. Rev. B **64**, 104416 (2001).
[19] K.J. Singh, S. Chaudhary, M.K. Chattopadhyay, M.A. Manekar, S.B. Roy, and P. Chaddah, Phys. Rev. B **65**, 094419 (2002).
[20] M. Manekar, S. Chaudhary, M.K. Chattopadhyay, K.J. Singh, S.B. Roy, and P. Chaddah, J. Phys.: Condens. Matter **14**, 4477 (2002).
[21] J.A. Mydosh, *Spin Glasses: An Experimental Introduction* (Taylor & Francis, London 1993).
[22] S.B Roy, A.K. Pradhan, and P. Chaddah, J. Phys.: Condens. Matter **6**, 5155 (1994); S.B. Roy, A.K. Pradhan, and P. Chaddah, Philos. Mag. B **71**, 97 (1995); S.B. Roy, A.K. Pradhan, and P. Chaddah, Physica B **223-224**, 198 (1996); S.B. Roy, A.K. Pradhan, and P. Chaddah, Philos. Mag. B **75**, 303 (1997); S.B. Roy, A.K. Pradhan, P. Chaddah, and E.V. Sampathkumaran, J. Phys.: Condens. Matter **9**, 2465 (1997); S. Chaudhary, S.B. Roy, and P. Chaddah, J. Alloys Compd. **326**, 112 (2001).
[23] P.S. Anilkumar, P.A. Joy, S.K. Date, Bull. Mater. Sci. **23**, 97 (2000); P.A. Joy, P.S. Anilkumar, and S.K. Date, J. Phys.: Condens. Matter **10**, 11 049 (1998).
[24] P.M. Chaikin and T.C. Lubensky, in *Principles of Condensed Matter Physics* (Cambridge University Press, Cambridge, England, 1995).
[25] P. Chaddah and S.B. Roy, Phys. Rev. B **60**, 11 926 (1999).
[26] R.M. White and T.H. Geballe, in *Long Range Order in Solids* (Academic, New York, 1979).